Acta Biomaterialia 10 (2014) 4928–4938

Contents lists available at ScienceDirect

Acta Biomaterialia

journal homepage: www.elsevier.com/locate/actabiomat

A two-component pre-seeded dermal–epidermal scaffold

I.P. Monteiro [a,b,c,d], D. Gabriel [a,b], B.P. Timko [a,b], M. Hashimoto [a,b], S. Karajanagi [b,e], R. Tong [a,b], A.P. Marques [c,d], R.L. Reis [c,d], D.S. Kohane [a,b,*]

[a] Laboratory for Biomaterials and Drug Delivery, Department of Anesthesiology, Division of Critical Care Medicine, Children's Hospital Boston, Harvard Medical School, 300 Longwood Avenue, Boston, MA 02115, USA
[b] Department of Chemical Engineering, Massachusetts Institute of Technology, 77 Massachusetts Avenue, Cambridge, MA 02139, USA
[c] 3B's Research Group – Biomaterials, Biodegradables and Biomimetics, University of Minho, Headquarters of the European Institute of Excellence on Tissue Engineering and Regenerative Medicine, AvePark, 4806-909 Taipas, Guimarães, Portugal
[d] ICVS/3B's – PT Government Associate Laboratory University of Minho, Braga/Guimarães, Portugal
[e] Department of Surgery, Massachusetts General Hospital, Harvard Medical School, 55 Fruit Street, Boston, MA 02114, USA

ARTICLE INFO

Article history:
Received 25 April 2014
Received in revised form 18 August 2014
Accepted 25 August 2014
Available online 1 September 2014

Keywords:
Skin defects
Bilayered
Hyaluronic acid
Amine–aldehyde bonding

ABSTRACT

We have developed a bilayered dermal–epidermal scaffold for application in the treatment of full-thickness skin defects. The dermal component gels in situ and adapts to the lesion shape, delivering human dermal fibroblasts in a matrix of fibrin and cross-linked hyaluronic acid modified with a cell adhesion-promoting peptide. Fibroblasts were able to form a tridimensional matrix due to material features such as tailored mechanical properties, presence of protease-degradable elements and cell-binding ligands. The epidermal component is a robust membrane containing cross-linked hyaluronic acid and poly-L-lysine, on which keratinocytes were able to attach and to form a monolayer. Amine–aldehyde bonding at the interface between the two components allows the formation of a tightly bound composite scaffold. Both parts of the scaffold were designed to provide cell-type-specific cues to allow for cell proliferation and form a construct that mimics the skin environment.

1. Introduction

Adult skin is composed of the epidermis and dermis: the top layer of the epidermis is the stratum corneum, a thin, water-tight layer of dead, flattened cells covering rapidly dividing keratinocytes beneath. The underlying thicker dermis is a complex association of fibroblasts, blood vessels, nerve fibers and lymphatics embedded in the extracellular matrix (ECM) [1,2]. The dermis and epidermis are connected by the dermal–epidermal junction, which is composed of the basal cell plasma membrane, a multilayered structure which contains hemidesmosomes and which provides epidermal–dermal adherence and mechanical support for the epidermis, and acts as a barrier to the transfer of cells and of some large molecules across the junction [3]. Skin injury from thermal trauma and other causes is an important public health problem [4]; third-degree burns, which involve damage to epidermal, dermal and deeper layers, cause the hospitalization of hundreds of thousands of patients every year [5]. In full-thickness defects, particularly in lesions more than 4 cm across and 0.4 mm deep, natural healing is inadequate due to a lack of remaining regenerative elements [1,6–8], and grafting of skin is likely to be necessary [6]. Common skin grafting techniques involve transplanting split-thickness skin [9], which contains the epidermis and a variable fraction of the underlying dermis. The availability of donor skin is a limiting factor requiring the development of engineered dermo-epidermal skin substitutes analogous to full-thickness autologous skin [9].

Extant commercially available skin substitutes have limitations. The only commercially available bilayered scaffold skin substitute (combination of Laserskin® and Hyalograft3-D™) requires multiple procedures [4,10–12]. Collagen-based skin substitutes containing dermal fibroblasts and keratinocytes suffer from limited anchorage and keratinocyte survival, poor structural integrity and incomplete cell differentiation [13,14].

Patients could benefit greatly from a scaffold which mimics the two-compartment structure of skin and that could be easily handled and applied, rapidly adapting to complex three-dimensional lesion sites and composed of materials that promote angiogenesis (fibrin [15–17] and hyaluronic acid [18]). Such scaffolds should be applicable to any depth or shape of lesion, and should allow the

* Corresponding author at: Laboratory for Biomaterials and Drug Delivery, Department of Anesthesiology, Division of Critical Care Medicine, Children's Hospital Boston, Harvard Medical School, 300 Longwood Avenue, Boston, MA 02115, USA. Tel.: +1 617 919 2364; fax: +1 617 730 0453.
E-mail address: daniel.kohane@childrens.harvard.edu (D.S. Kohane).

http://dx.doi.org/10.1016/j.actbio.2014.08.029
1742-7061/

co-culture of cells by furnishing tailored biological and mechanical properties for each compartment, speeding up the healing process by the simultaneous regeneration of dermis and epidermis [13,19]. We have designed an in situ forming dermal–epidermal scaffold which is adaptable to differing lesion shapes, and is designed to mimic the bilayer structure of human skin while providing instructive cues for cell adhesion, migration and proliferation. The dermal component consists of fibrin and cross-linked hyaluronic acid (HAX), modified with a peptide derived from the cell adhesion molecule fibronectin to improve cell attachment. The dermal layer provides a porous, proteolytically degradable bioactive scaffold where dermal fibroblasts can proliferate and form a tridimensional matrix. The epidermal component is a mechanically robust membrane of HAX combined with poly-L-lysine (PLL) to provide anchoring to the dermal layer via aldehyde–amine interactions and coated by laminin-5 to enhance the attachment of keratinocytes (Fig. 1). In a clinical context, the dermal hydrogel with fibroblasts would be injected into the lesion, crosslinking in situ and adapting to the lesion shape in seconds, with immediate subsequent application of the epidermal membrane seeded with keratinocytes on the top surface. The free aldehyde groups of the dermal hydrogel would react covalently with amines of the PLL-modified epidermal hyaluronic acid (HA) membrane layer to create a single structure in situ.

2. Materials and methods

2.1. Materials

Sodium hyaluronate (MW 351–600 kDa and 1.2–1.8 MDa) was purchased from LifeCore Biomedical (Chaska, MN, USA). Adipic acid dihydrazide (ADH), 1-ethyl-3-[3-(dimethylamino)-propyl]carbodiimide (EDC), sodium hydroxide, hydrochloric acid, hydroxybenzotriazole, sodium periodate, ethylene glycol, Dowex®

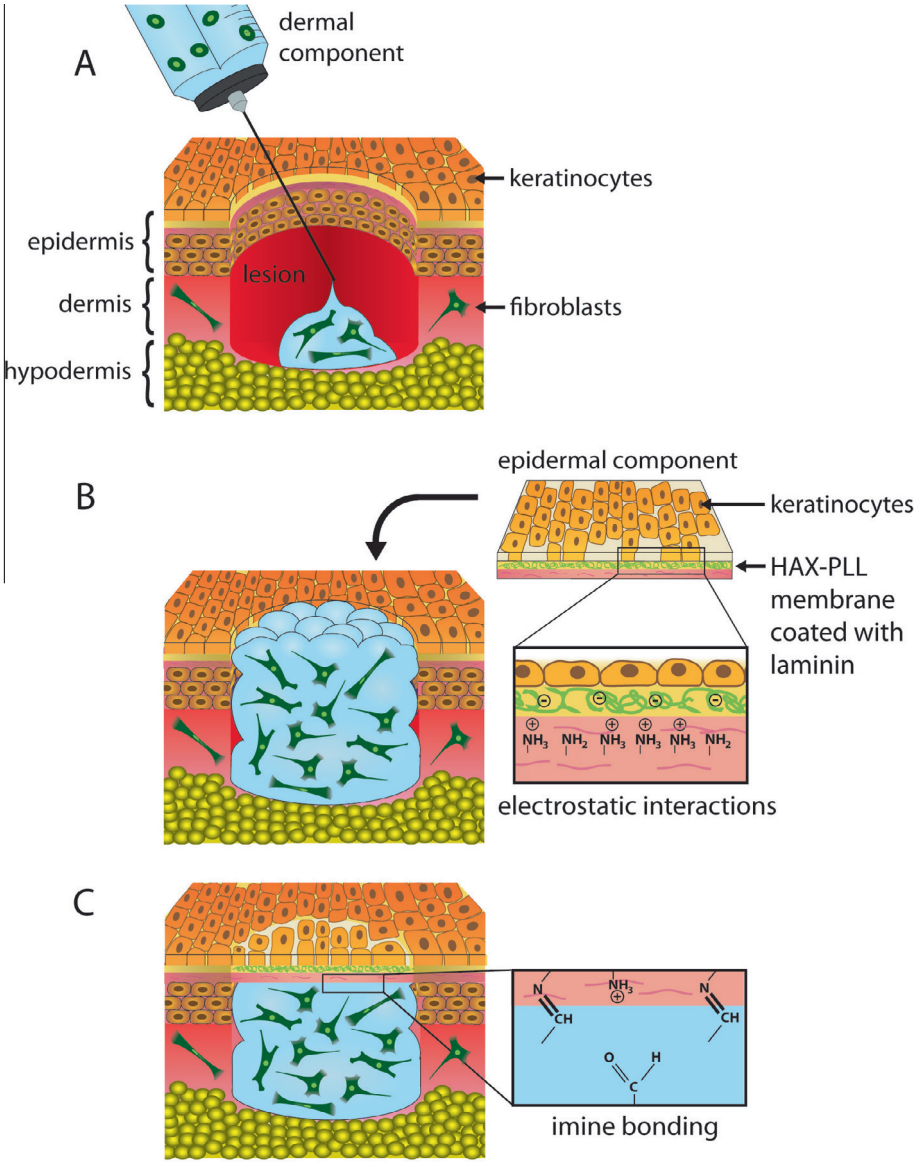

Fig. 1. Schematic of the bilayered epidermal–dermal scaffold. (A) An in situ gelling dermal component (blue) containing human dermal fibroblasts (green) is applied into the lesion and adapts to its shape. (B) A thin epidermal membrane pre-seeded with keratinocytes is applied on top of the dermal layer. Inset: negatively charged laminin (light green) interacts with positively charged PLL in the membrane (pink). (C) The epidermal layer protects the dermal part from dehydration and infection. Inset: free amines of the epidermal component (pink) react with aldehydes in the dermal component (blue) to form covalent imine interactions which glue the two components together to form a single composite scaffold.

50WX8–400 resin, N-hydroxysulfosuccinimide (S-NHS), 4′,6-diamidino-2-phenylindole (DAPI), phalloidin, poly-L-lysine (PLL; MW 4000–15,000 Da), fluorescein isothiocyanate (FITC)-labeled PLL (MW 30–70 kDa), thrombin (300 NIH units mg^{-1}), fibrinogen from human plasma, anhydrous N,N-dimethylformamide (99.8%), paraformaldehyde (PFA), hyaluronidase and Triton™ X-100 were obtained from Sigma (St. Louis, MO, USA). Dialysis membranes (MW cutoff 3.5 kDa) were purchased from Spectrum Labs (Rancho Dominguez, CA, USA). The fibronectin active fragment, Gly–Arg–Gly–Asp–Ser, was purchased from Peptides International (Louisville, KY, USA). Laminin-5 protein, mouse monoclonal to cytokeratin 14 and goat polyclonal secondary antibody to mouse IgG (H&L) (FITC) were obtained from Abcam (Cambridge, MA, USA). Amicon® centrifugal filter units, Transwell® with 3.0 μm pores and Millicell® cell culture polycarbonate inserts with 0.4 μm pores, 12 mm filter diameter, were obtained from Millipore (Billerica, MA, USA). Biopsy punches were obtained from HealthLink (Jacksonville, FL, USA). A cell strainer with a 100 μm pore size was purchased from BD Biosciences (Franklin Lakes, NJ, USA). Alexa Fluor®-647 hydrazide, LIVE/DEAD® assay, alamarBlue® assay, Quant-iT™ PicoGreen® dsDNA kit, phosphate-buffered saline (PBS), human keratinocytes and human fibroblasts, Dulbecco's modified Eagle's medium (DMEM), fetal bovine serum (FBS) and penicillin–streptomycin (Pen/Strept) were obtained from Invitrogen Life Technologies (Carlsbad, CA, USA). Progenitor cell target medium (CnT-57) was obtained from CELLnTEC (Bern, Switzerland). Double-barrel syringes were obtained from Baxter (Deerfield, IL, USA). Polytetrafluoroethylene (Teflon®) molds were obtained from VWR International (Chicago, IL, USA).

2.2. Cell culture

Human keratinocytes were expanded in CnT-57 medium supplemented with 1% Pen/Strept. Fourth passage keratinocytes were used in experiments. Human primary skin fibroblasts were expanded in DMEM supplemented with 10% FBS and 1% Pen/Strep. Fibroblasts used for experiments were at passage three. Cells were passaged using standard protocols and cultured in a 5% CO_2 incubator at 37 °C.

2.3. HA modification

High MW HA (1.2–1.8 MDa) and low MW HA (351–600 kDa) were functionalized respectively with aldehyde (HA-CHO) and hydrazide (HA-ADH) groups, as described previously [20,21]. The HA modification into HA-CHO or HA-ADH was confirmed using proton nuclear magnetic resonance (^{1}H NMR).

2.4. Activation of HA-CHO by the fibronectin active fragment

Prior to modification with the fibronectin active fragment, HA-CHO polymer was ion exchanged overnight in Dowex® 50 W X8-400 resin. For this, 40 mg of the HA-CHO was dissolved in PBS. The carboxylic acid group on HA-CHO was activated by S-NHS (3 equivalents). The reaction was mediated by ECD-HCl (3 equiv) for 30 min. After filtration using Amicon® units (MW cutoff 10 kDa), 5 mg of the cell adhesion peptide fibronectin active fragment (MW 490.47 Da), was conjugated to the activated HA-CHO through amide bond formation. After the reaction, the HA-GRGDS solution was purified by exhaustive dialysis (MW cutoff 3.5 kDa), frozen in liquid nitrogen and lyophilized. The change in the molecular weight from the HA-CHO to the HA-CHO-GRGDS was verified by gel permeation chromatography (GPC). The degree of peptide modification per available carboxylic acid was determined by ^{1}H NMR.

2.5. Preparation of the dermal component for fibroblast culture

Solutions of HA-CHO-GRGDS (40 mg ml^{-1}), thrombin (6.25 mg ml^{-1}, 300 NIH units mg^{-1}), HA-ADH (40 mg ml^{-1}) and fibrinogen (83.4 mg ml^{-1}) were prepared in DMEM containing 10% FBS. Two independent mixtures were created: (i) 200 μl of HA-CHO-GRGDS (40 mg ml^{-1}) was mixed with 200 μl thrombin; and (ii) 200,000 human fibroblasts in 200 μl of the HA-ADH (40 mg ml^{-1}) were mixed with 200 μl fibrinogen. A double-barrel syringe was used to mix the solutions and the formed gel was poured in a 48-well plate.

2.6. Gelation time of the dermal component

Equal volumes (200 μl) of the HA-CHO-GRGDS-thrombin and the HA-ADH-fibrinogen were mixed and stirred in a glass vial with a stirring bar until formation of a solid gel (the dermal component). The gelation time was defined as the time required to create the solid globule, which was completely separated from the bottom of three glass vials.

2.7. Degradation studies

Degradation studies were carried out by incubating four samples of the dermal hydrogel (after reaching the swelling equilibrium) in PBS, in the presence of 10 U ml^{-1} hyaluronidase, in an orbital shaker at 37 °C. Samples were placed in transwells to facilitate handling. Every day, they were blotted dry and weighed, and the hyaluronidase solution was replaced. The percentage of weight loss was determined by dividing the measured weight at each time point (W_t) by the initial weight after swelling to equilibrium in PBS (W_i): % weight = $W_t/W_i \times 100$. Scanning electron microscopy (SEM) images of the samples were obtained after freeze-drying.

2.8. SEM and pore size determination

The morphology of the freeze-dried samples was observed under a 5600LV scanning electron microscope (JEOL, Tokyo, Japan), after sputter-coating them with an ultrathin (10 nm) layer of gold using a Hummer 6.2 Sputtering System from Anatech Ltd (Hayward, CA, USA). The pore size was determined using the measure-length function in the AxioVision Software (Zeiss, Germany). When the pores were not exactly round, the length was measured as the greatest diameter in each pore.

2.9. Determination of the mechanical properties of the dermal component

The viscoelastic shear properties of the gels HAX-GRGDS, fibrin/HAX-GRGDS and fibrin were measured at low frequencies using an AR-2000 rheometer (TA Instruments, Inc., New Castle, Delaware, USA). Samples were fully swollen in PBS prior to measurements. A plate-and-plate (parallel plate) geometry was used to apply oscillatory shear to hydrogel samples using a stainless steel plate (20 mm diameter) at 25 °C. Gel disks (1 ml total volume) were made in a 12-well plate and then cut with a 12 mm biopsy punch. The fully swollen gels were placed between the two plates so that a gap of 1000 or 1800 μm was maintained between the two plates. Strain sweep tests were done to ensure that the shear property measurements were done in the linear region of the stress–strain curve. The viscoelastic shear properties are independent of the strain applied in the linear region. A target shear strain value was identified by measuring the viscoelastic shear properties as a function of strain applied (0.6% strain was used to measure the shear properties). Measurements of the shear properties were then made by systematically varying the frequency from 1 to 10 Hz. The

elastic shear modulus (G') at 10 Hz was used as a measure of the mechanical properties of the hydrogels used in this study.

2.10. Preparation of the epidermal component for keratinocytes' culture

HA-CHO (40 mg ml^{-1} in PBS) and HA-ADH (40 mg ml^{-1} in PBS) were mixed with a PLL solution (1 mg ml^{-1}) at an experimentally optimized ratio of 2:2:1 and poured into a polytetrafluoroethylene (Teflon®) mold. Because HA is a polyanion and PLL is a polycation, its complexation, followed by the solvent evaporation at room temperature (RT), allowed the creation of a stable membrane. After drying, the membrane easily detached from the mold surface. For further surface modification with (FITC-labeled)-PLL, they were immersed in a solution of 11 mg ml^{-1} S-NHS, 50 mg ml^{-1} EDC-HCl and 5 mg ml^{-1} (FITC-labeled)-PLL, and left to react for 18 h. After thorough washing with PBS, a 8 mm diameter biopsy punch was used to create small membranes. For cell culture, these membranes were coated with laminin-5 (1 μg ml^{-1}) and left overnight in the humidified incubator. The membranes were placed in cell culture porous inserts. The next day, 1×10^5 keratinocytes in 400 μl of CnT-57 medium were seeded into the membranes.

2.11. Force measurements of the epidermal component

Young's modulus was measured using an atomic force microscope (Model MFP-3-D, Asylum Research, Santa Barbara, CA, USA) with an antimony-doped silicon cantilever (f_0 = 50–100 kHz, k = 1–5 N m^{-1}; Model FESP, Bruker AFM Probes, Camarillo, CA, USA). Data were collected and analyzed using a proprietary procedure running in Igor Pro software (WaveMetrics, Inc., Portland OR, USA). Hydrogel samples were clamped onto a glass slide and submerged in PBS. Force curves were collected in contact mode. Young's modulus was calculated by fitting the linear portion of force curves with the Hertz model.

2.12. Adhesion studies

As a preliminary study to assess the adhesion between the epidermal and the dermal layer, 8 mg of the HA-CHO was reacted with 0.48 mg Alexa Fluor®-647 hydrazide in a PBS buffer for 4 h at RT. The HA-Alexa Fluor®-647 conjugate was then purified by dialysis (MW cutoff 30 kDa) for 2 days. To create a green fluorescent membrane, 30% PLL was replaced by FITC-labeled polymer to prepare the epidermal membrane.

In order to quantify the adhesion, a 12 mm biopsy punch was used to cut both the membrane and the dermal substitute. Membranes containing the PLL modification or not and the dermal substitutes were glued separately with Super Glue to 14 mm metal tubular fittings, providing a flat and stable presentation. The tubular fittings were inserted into the upper and lower arms of the mechanical testing apparatus Instron® (Norwood, MA, USA) configured for tensile testing, with the membranes and the gels facing each other. The membranes were kept in contact with the dermal component for 10 min under a 1.3 N setting force in order to cure. The tissue–adhesive interface was displaced at a rate of 0.05 mm min^{-1} until complete separation occurred. The maximal force measured by the 20 N load cell prior to interface failure was recorded as the adhesion force of the tested material. To test if covalent bonding of aldehydes in the dermal component with amines of the epidermal component increased the force required to separate the two layers, we blocked aldehyde groups with adipic acid dihydrazide (5 mg ml^{-1}) for 15 min prior to the experiment.

2.13. alamarBlue® assay

The alamarBlue® proliferation assay was performed according to the manufacturer's instructions [22]. Briefly, the stock solution was diluted in cell culture medium at a 1:10 ratio, then 1 ml of this solution was added to the scaffolds in a 48-well plate and incubated for 4 h at 37 °C in the dark. Next, 100 μl of this solution was transferred into a 96-well plate and the fluorescence was read at 600 nm using excitation at 570 nm. The background fluorescence was subtracted from all values.

2.14. DNA quantification

Cellular DNA was quantified using the PicoGreen® dsDNA kit, according to the manufacturer instructions [23]. The cell content was removed from the scaffolds by freezing them at −80 °C and subsequent sonication. The fluorescence of samples and standards was measured using 485 nm excitation light at an emission wavelength of 528 nm. The DNA concentration was extrapolated from a previously established standard curve.

2.15. LIVE/DEAD® assay

The LIVE/DEAD® cell viability kit for mammalian cells [24] was used to visualize cell viability after different periods of culture. Calcein-AM and ethidium homodimer-1 were dissolved in PBS at concentrations of 2 and 4 μM, respectively. Keratinocytes and fibroblast were incubated with this solution for 20 min. After washing twice with PBS, the fluorescence of the cells was observed using a Zeiss 710 confocal microscope (Germany).

2.16. Immunocytochemistry

For immunocytochemistry, cells were fixed overnight at 4 °C in 4% PFA dissolved in PBS. After washing twice with PBS, cells were permeabilized using 0.25% Triton™ X-100. In order to block non-specific antibody binding, cells were incubated for 30 min at RT with 1% BSA in PBS. The BSA solution was removed and the cells were incubated in cytokeratin-14 (1:400) overnight at 4 °C. After washing three times with PBS, the secondary antibody goat polyclonal secondary antibody to mouse IgG (H&L) (FITC) was added in the concentration 1:4000. After washing three times, the actin filaments were stained with phalloidin (1:200) for 20 min at RT and the cell nuclei were stained with DAPI (0.1 μg ml^{-1}) for 1 min, also at RT. Cells were then observed under a fluorescence microscope (Zeiss, Germany).

2.17. Histology

Samples with cells were fixed in 4% PFA overnight at 4 °C and left in 70% ethanol. Specimens were embedded in paraffin wax and sectioned into 6 μm sections, which were routinely processed for hematoxylin and eosin staining (H&E).

2.18. Data analysis

Experiments were performed using four samples per condition. Data are presented as mean ± standard deviations, with n = 4 for each group, compared by one-way analysis of variance and Tukey's post hoc multiple comparison test or by an unpaired t-test using GraphPad Prism 5® software (La Jolla, CA, USA).

3. Results and discussion

We have developed an epidermal–dermal skin substitute composed of (i) an in situ gelling dermal component, which adapts to the shape of the lesion, and (ii) an epidermal component, which anchors to and protects the dermal component. The dermal substitute contains human dermal fibroblasts three-dimensionally distributed in a fibrin/HAX-GRGDS gel. The epidermal substitute is a membrane composed of HAX and PLL, which anchors to the dermal component via aldehyde–amine crosslinking, forming a single composite structure (Fig. 1).

3.1. Dermal component

A composite hydrogel providing appropriate mechanical properties, protease-degradable elements and cell-binding ligands was designed to mimic the dynamic network of the dermal ECM, consisting of protein fibers and polysaccharides [25,26]. HA was chosen as the polymeric basis for the scaffold matrix because it is biodegradable, and promotes migration, differentiation and proliferation of fibroblasts and endothelial cells [27,28]. HA enhances angiogenesis and the production of ECM components during wound healing, supporting regeneration and the scarless healing of wounds [29,30]. Despite these useful properties, cells do not easily attach to HA, because of its hydrophilicity [31–33]. Conjugation of RGD peptides can improve cell adhesion to HA [34].

We modified the HA polymer for the dermal component with the fibronectin-derived peptide GRGDS [35–37] (Fig. 2A). The successful conjugation of the peptide sequence to the activated carboxylic acid of the aldehyde modified HA (HA-CHO, to be reacted with HA-ADH in order to form HAX) was confirmed by NMR (Fig. 2B) and by gel permeation chromatography (Fig. 2C). Comparison of the integrated ^{1}H NMR signals of the methyl protons of HA-CHO (chemical shift ~1.8 ppm in NMR spectrum) with the methylene protons on the side chains of arginine (R) and aspartic acid (D) in the GRGDS peptide (chemical shift at ~2.6–2.8 ppm in spectrum) showed that the degree of HA carboxylic acid modification with the peptide was approximately 10%. The modification of HA-CHO with GRGDS decreased its retention time on GPC, indicating that its molecular weight was increased (Fig. 2C). The peak did not broaden and there were no detectable new peaks with shorter retention times, suggesting that the dispersity of the polymer did not change significantly and that no detectable amounts of high-molecular-weight cross-linked polymer products resulted from the conjugation reaction.

HA was also modified with adipic hydrazide (HA-ADH), to allow in situ cross-linking with HA-CHO (forming cross-linked HA, HAX) upon application with a double-barrel syringe. Both HA-CHO and HA-ADH were modified using established protocols [38–40]. The degree of ADH incorporation in HA was verified by ^{1}H NMR spectroscopy and the percentage of oxidation of HA was quantified by measuring the number of aldehyde groups in the polymer using *t*-butyl carbazate [20,41,42].

Fibrin (formed from the reaction of fibrinogen with thrombin) was incorporated into the dermal component to confer protease degradability [43,44] and to modulate gel stiffness in order to facilitate cell penetration [45,46]. Solutions of fibrinogen/HA-ADH (1:1 by volume) were mixed with thrombin/HA-CHO-GRGDS (1:1 by volume). Upon mixing, the two solutions formed a homogeneous cross-linked hydrogel (fibrin/HAX-GRGDS, the dermal component), with a gelation time of 33 ± 3 s. The fibrin/HAX-GRGDS gel adopted the shape of the mold into which it was cast (Fig. 3A and B); by

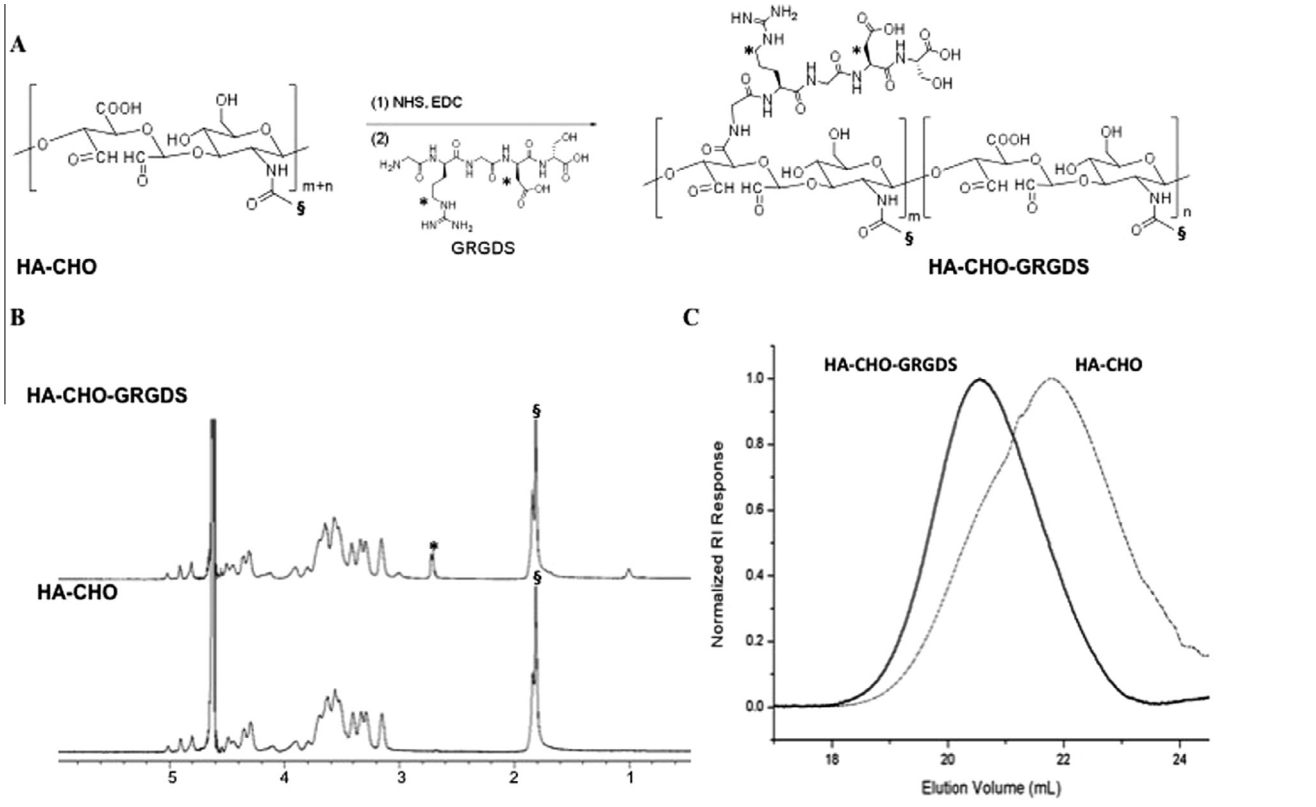

Fig. 2. Peptide conjugation to HA-CHO. (A) Chemical structure of HA-CHO, the fibronectin-derived peptide sequence, GRGDS, and the peptide-modified HA-CHO-GRGDS (* denotes methylene protons in the side chains of arginine and aspartate in the GRGDS peptide, corresponding to the asterisked peak at ~2.6–2.8 ppm in panel B; § denotes the methyl protons of HA-CHO at 1.8 ppm). (B) ^{1}H-NMR spectra showing that approximately 10% the available carboxylic acids in HA were modified with the peptide (* indicates the conjugated peptide). (C) GPC showing an increase in molecular weight of the HA-CHO-GRGDS conjugate relative to the molecular weight of HA-CHO.

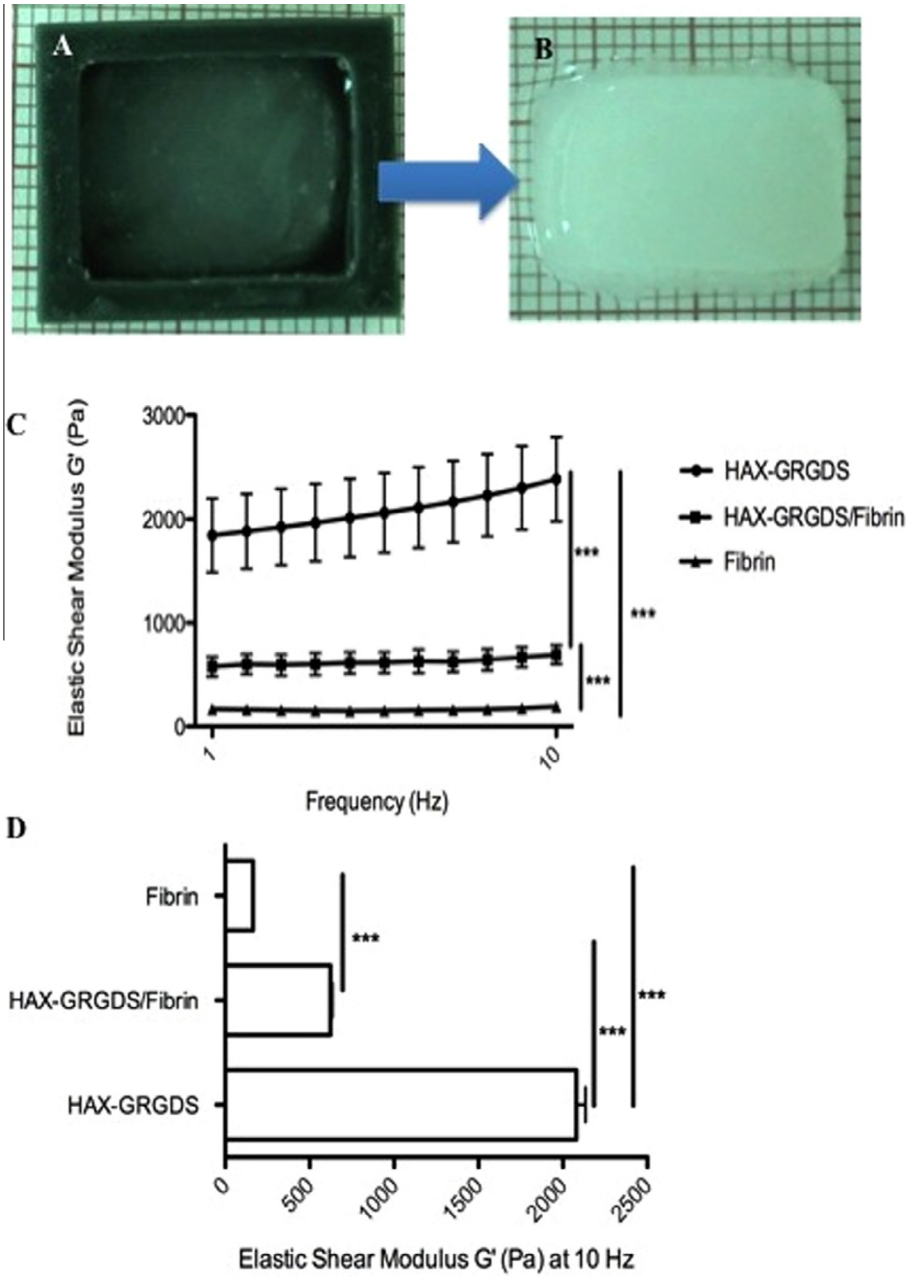

Fig. 3. Dermal component. (A, B) The dermal component maintains the shape of the mold in which it was cast. (C, D) Viscoelastic shear properties of the different hydrogels. (C) Elastic shear properties obtained by varying the frequency from 1 to 10 Hz. (D) The elastic shear modulus (G') at 10 Hz. Data are means ± standard deviations, $n = 4$ for each group, compared by an unpaired t-test (***$p < 0.0001$).

gross examination, the fibrin/HAX-GRGDS gel had a reduced stiffness and brittleness compared to the cross-linked gel (HAX). Mechanical studies of the fully swollen gels (Fig. 3C and D) allowed the calculation of the shear modulus (G) as 2413 ± 399 Pa for HAX-GRGDS, 694 ± 93 Pa for fibrin/HAX-GRGDS and 196 ± 34 Pa for fibrin. G has two components – storage (elastic) shear modulus (G') and loss (viscous) shear modulus (G'') – and is defined by Eq. (1):

$$G = \sqrt{G' \times G' + G'' \times G''} \quad (1)$$

The G' of fully swollen HAX-GRGDS-, fibrin/HAX-GRGDS- and fibrin hydrogels was measured at 10 Hz, giving values of 2384 ± 404 Pa for HAX-GRGDS, 694 ± 93 Pa for fibrin/HAX-GRGDS and 193 ± 35 Pa for fibrin. It has been reported that the matrix can act as a barrier to cells in 3-D culture at G' higher than 1200 Pa, even in the presence of protease-degradable elements or cell–integrin binding sites [47]. The higher the G', the more difficult it is for fibroblasts to spread, proliferate and migrate [47]. G can be correlated with Young's modulus according to Eq. (2) [48]:

$$E = 2 \times G \times (1 + \upsilon) \quad (2)$$

in which E is Young's modulus, G is the shear modulus and υ is Poisson's ratio. A rough estimate of E may be obtained from G by assuming a Poisson's ratio of 0.5 for a fully swollen hydrogel, such as the ones reported here [49]. The calculated values of E for HAX-GRDS, fibrin/HAX-GRGDS and fibrin were 7239 ± 1197, 2083 ± 279 and 587 ± 103 Pa, respectively. The values of E obtained for both the fibrin/HAX-GRGDS and the fibrin hydrogel are within the range of values for soft tissues in the human body [50]. The reduced stiffness

after the incorporation of fibrin into HAX-GRDS hydrogel may help cells to displace polymer chains and make room for their movement [51]. The fibrin gels were the softest, and were not elastic or stiff enough to maintain their form during oscillatory shear mechanical testing. In fact, low mechanical stiffness has been a limiting factor for the use of scaffolds based solely on fibrin and is a major reason for its frequent combination with other scaffold materials [52].

Fibrin/HAX-GRGDS scaffolds with a diameter of 10 mm and a thickness of 5 mm were prepared, containing 200,000 human dermal fibroblasts per scaffold. Cells were suspended in the fibrinogen/HA-ADH prior to mixing with thrombin/HA-CHO-GRGDS (1:1 by volume) to assure the homogeneous distribution of the cells within the scaffold. The cells showed continuous proliferation over 9 days, as assessed by the alamarBlue® assay [22] (Fig. 4A) and by measuring the increase in the double-stranded DNA content [23] (Fig. 4B). LIVE/DEAD® staining and subsequent fluorescence microscopy demonstrated that the fibroblasts were able to grow three-dimensionally throughout the scaffold. Moreover, the negligible number of dead cells indicated that the material had minimal toxic effects on the cells. Twenty-four hours after seeding (day 1, Fig. 4C), cells were alive and spherical; by day 3, they showed the characteristic spindle shape of dermal fibroblasts (Fig. 4D). On days 6 (Fig. 4E) and 9 (Fig. 4F), fibroblasts had proliferated and spread extensively. Photomicrographs of the mid-portions of H&E-stained horizontal sections of the dermal component confirmed that the fibroblasts were distributed throughout (Fig. A1). Cells cultured in HAX or fibrin/HAX hydrogels without the GRGDS modification resulted in comparable numbers of calcein-stained viable cells per scaffold (Fig. A2A and B), but the cells did not adopt the characteristic spindle shape of fibroblasts. Instead, fibroblasts

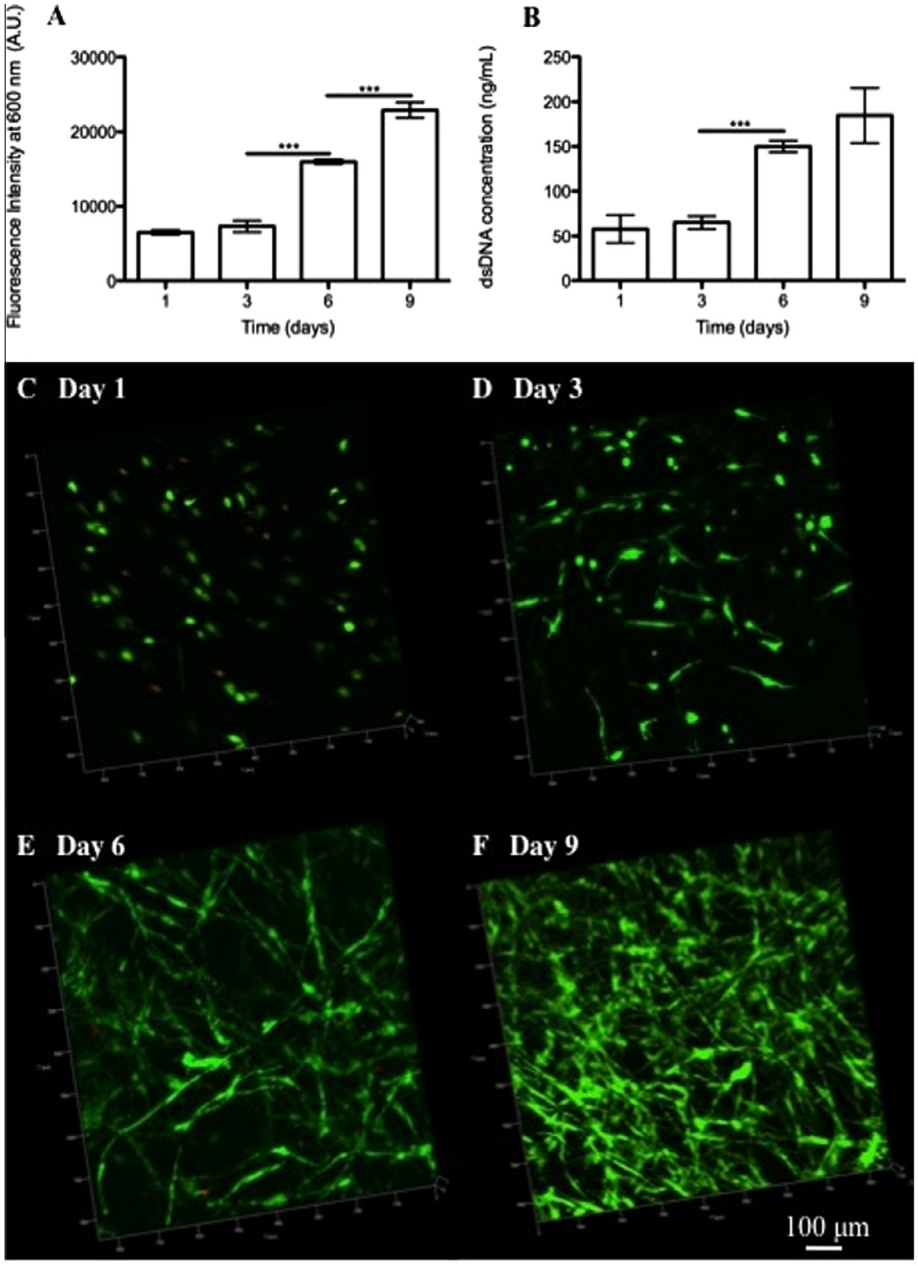

Fig. 4. Cell proliferation in the dermal substitute. (A) alamarBlue® fluorescence over time. (B) dsDNA concentration over time. Data are means ± standard deviations, $n = 4$ for each condition, compared by an unpaired t-test (***$p < 0.0001$). (C–F) Confocal fluorescence images of dermal fibroblasts growing in the dermal gel component at various time points. Green (calcein-AM) and red (propidium iodine) stained cells are viable and dead, respectively.

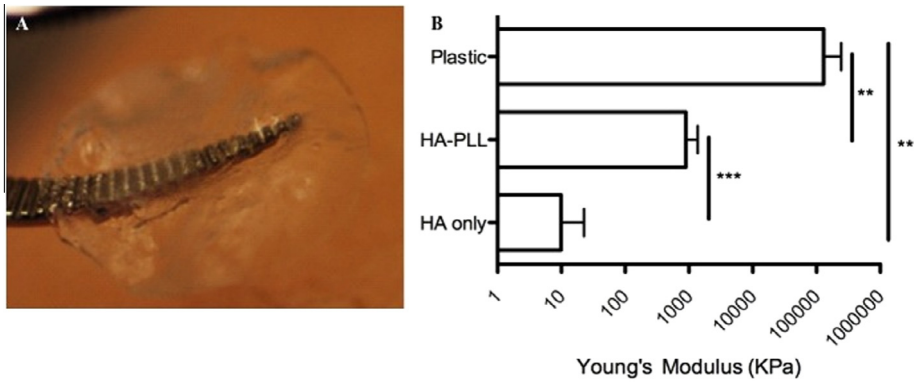

Fig. 5. Epidermal component. (A) The epidermal component (HAX-PLL), held with one tine of a pair of forceps. (B) Young's modulus of membranes, determined by atomic force microscopy; note the log scale on the *x*-axis. The membranes were made of HAX or cross-linked HA with PLL (HAX-PLL, i.e. the epidermal component). Values are means ± standard deviations, $n = 4$, compared by an unpaired *t*-test (***$p < 0.0001$).

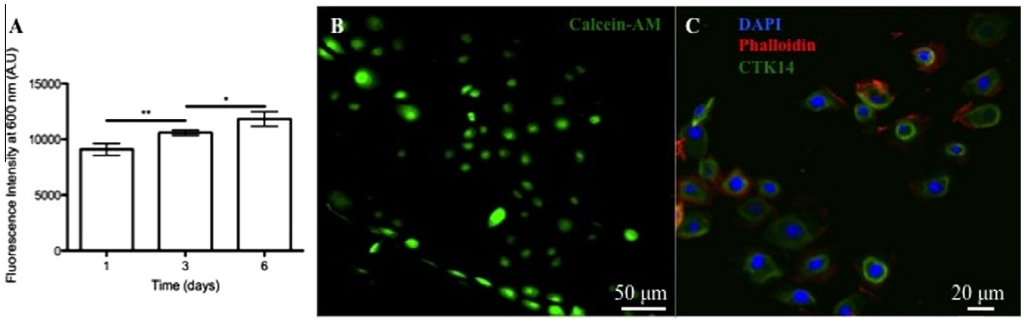

Fig. 6. Cell growth on the laminin-coated epidermal component. (A) alamarBlue® fluorescence increased from day 1 to day 6. Values are means ± standard deviations, $n = 4$, compared by an unpaired *t*-test (*$p = 0.012$; **$p = 0.002$). (B) LIVE/DEAD® assay at day 3 showing healthy keratinocytes in green, with a typical cuboidal morphology. (C) Cell staining showing cytokeratin-14 (green), a specific marker of epithelial basal keratinocytes at an early stage of differentiation. Phalloidin was used to stain actin filaments (red). Nuclei were stained with DAPI (blue).

adopted a rounded shape and tended to form cell aggregates. In HAX-GRGDS gels (in the absence of fibrin), only sparse rounded cells were observed (Fig. A2C), despite the presence of cell attachment ligands. Previous reports [34,53] suggest that RGD-based cell attachment ligands, protease-degradable elements and adequate matrix stiffness all contribute to morphological changes, such as acquiring a spindle shape and increased cell surface area [47]. Our findings are consistent with this view. Studies of degradation in hyaluronidase showed that the hydrogel degraded over 11 days (Fig. A3A–O).

3.2. Epidermal component

The epidermal component was designed to deliver epidermal keratinocytes to the wound site, allowing rapid re-epithelialization of a full-thickness skin defect and protecting the dermal layer from dehydration, mechanical disruption and infection. Dermal–epidermal interactions promote the proliferation of and the re-epithelialization by keratinocytes [4]. Membranes (HAX-PLL) were obtained by mixing 1 ml of PLL (1 mg ml^{-1}) into 2 ml of HA-CHO (40 mg ml^{-1}) and then adding 2 ml of HA-ADH (40 mg ml^{-1}). Hydrogel mixtures were left in polytetrafluoroethylene (Teflon®) molds overnight and were then cut into 8 mm diameter discs (Fig. 5A). As shown by nanoindentation studies, the addition of PLL significantly increased the membranes' Young's moduli (E), making them stiffer (Fig. 5B). Free-standing membranes of HA (containing negatively charge carboxylic acids) and PLL (containing negatively charged amines) have been produced by electrostatic interaction between those polyelectrolytes [54]. To facilitate keratinocyte attachment, one surface of the HA-PLL membrane was coated with the most abundant component of the basement membrane, the protein laminin-5 [55,56]. Membranes without that coating showed very limited cell attachment (data not shown). Keratinocytes on the laminin-coated membranes attached and proliferated slowly, as assessed by the alamarBlue® assay (Fig. 6A), for the culture times of 1, 3 and 6 days. Fluorescence imaging of LIVE/DEAD® stained cells on those membranes showed that cells attached and formed typical colonies (Fig. 6B) [57]. Confocal images showed that keratinocytes expressed cytokeratin-14 (Fig. 6C), a keratin of the basal cells of all stratified squamous epithelia [58], indicating that the keratinocytes were in an early stage of differentiation, suitable for transplantation.

3.3. Composite bilayer

To form a bilayer composite, the epidermal component was placed on top of the dermal matrix immediately after its gelation. The keratinocytes are only seeded on the top of the epidermal component. The free aldehyde groups of the dermal hydrogel were intended to react covalently with amines of the PLL-modified epidermal HA membrane layer. This chemistry has been applied to create glues which bind to tissue amines in situ [59,60] or to cross-link cells with an aldehyde surface modification to amines on unmodified cells [61]. A piece of the composite with the approximate dimensions of 3 mm × 5 mm × 5 mm (H × L × W) was cut and imaged with the confocal microscope. Z-stacks performed at different *YX*-positions of the sample showed a close apposition of the two layers (i.e. the epidermal layer containing FITC-PLL (blue) placed on the dermal component containing HA-CHO covalently labeled with Alexa Fluor®-647 (purple); see Section 2) (Fig. 7A).

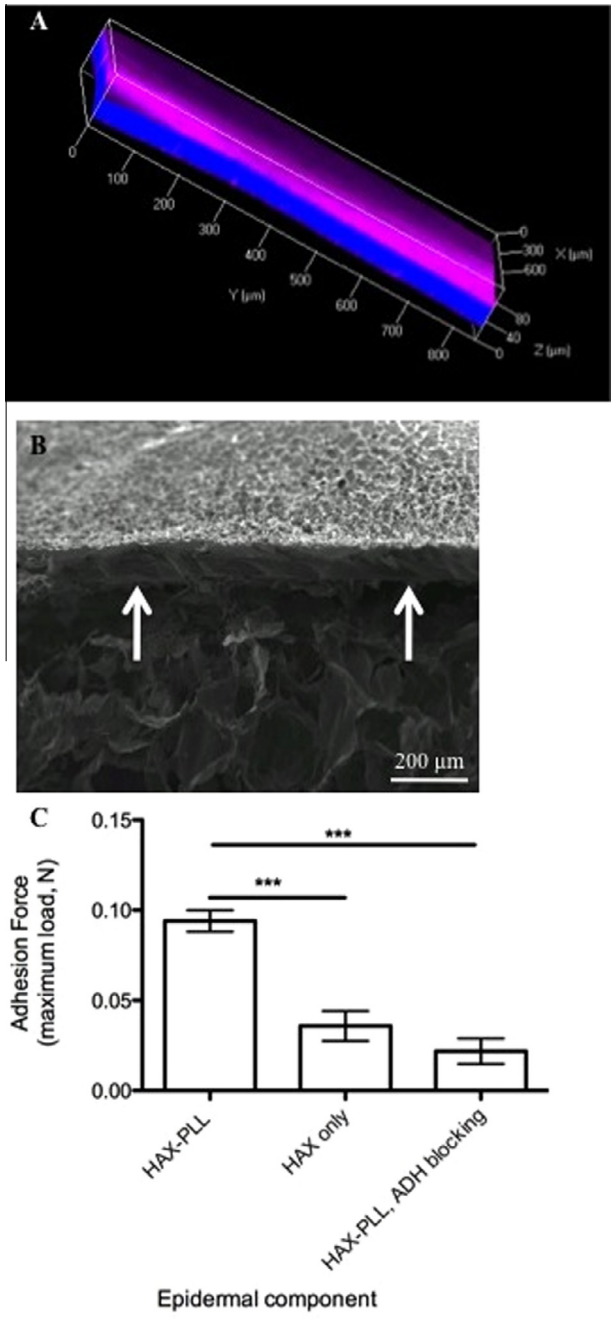

Fig. 7. Combination of the dermal component with the epidermal component. (A) Confocal fluorescence image of the two-component system: the membrane is labeled with FITC-PLL (blue) and the HA-CHO in the dermal component is covalently labeled with Alexa Fluor®-647 (purple). (B) SEM of the two-layered system with the dense epidermal membrane on top and the more porous dermal component on the bottom (arrows indicate the border between the epidermal and the dermal components). (C) Load required to separate the dermal gel from the epidermal membrane. HAX-PLL: adhesion force measured between an epidermal component containing free amines and a dermal component containing aldehydes. HAX only: adhesion force measured between an epidermal component without free amines (PLL) and a dermal component containing aldehydes. HAX-PLL, ADH blocking: conditions were as for HAX-PLL, but the aldehydes in the dermal compartment were blocked with adipic dihydrazide. Values are means ± standard deviations, $n = 4$, compared by an unpaired t-test (***$p < 0.0001$).

SEM of the composite structure showed a construct composed of two layers: a dense epidermal HAX-PLL membrane on top of a porous dermal scaffold (Fig. 7B). The small pore size (17.58 ± 6.49 μm) and flat surface of the epidermal component was designed to allow the formation of a cell monolayer with no cellular ingrowth, while allowing the diffusion of small molecules. The considerably bigger pores (177.49 ± 93.03 μm) of the dermal layer as well as the admixture of proteolytically degradable fibrin were designed to allow dermal fibroblasts to spread into the scaffold in three dimensions (Fig. 4C–F).

Mechanical testing (Fig. 7C) showed that a maximal force of 0.094 ± 0.006 N was necessary to detach the epidermal membrane made of HA and PLL from the dermal substitute, whereas only 0.036 ± 0.001 N was required for an epidermal membrane made of HA with no free amines. Capping of the free aldehydes in the dermal component with adipic acid dihydrazide prior to the mechanical testing resulted in values (0.021 ± 0.007 N) similar to those obtained with the membrane lacking free amines. These results suggest that the amine–aldehyde reaction created strong imine bonds between the two parts of the composite scaffold. This chemistry has been used to crosslink cells with an aldehyde surface modification to amines on unmodified cells [61], to create glues which bind to tissue amines in situ [20,21] and to enable in situ crosslinking hydrogels to be used in the peritoneum, without any toxic effects [40,62,63]. These tissue glues based on an aldehyde-modified dextran which reacts with free amines on the cell surface have approximately twice the adhesion strength of our system [64]. This may be because some of the aldehyde groups in our dermal system have reacted with the hydrazide-modified HA to form HAX-GRGDS and are not available for reaction with the PLL amines of the epidermal compartment.

Our approach offers a number of advantages over the current available skin substitutes: it uses materials that are approved for other applications by the Food and Drug Administration; it can be produced at an adequate cost and by reproducible methods; and it promotes angiogenesis (fibrin [15–17] and hyaluronic acid [18]).

4. Conclusion

We have developed a composite scaffold that combines a fibroblast-containing dermal matrix with a keratinocyte-containing epidermal membrane, linked together by amine–aldehyde interactions. Due to its in situ cross-linking ability, the dermal gel component is easy to apply and will conform to the shape of any lesion. The dermal component has the appropriate mechanical properties, cell adhesion sites and protease-degradable elements to allow the tridimensional spreading of human fibroblasts, forming a dermal matrix. The epidermal component is robust and allows the creation of a monolayer of keratinocytes. It will protect the dermal matrix from dehydration and infection. The composite bilayer described here holds potential as a skin replacement product that would allow establishment of both skin layers in a single procedure.

Notes

The authors declare no competing financial interest.

Acknowledgements

D.S.K. acknowledges funding from the Biotechnology Research Endowment from the Department of Anesthesiology at Boston Children's Hospital. I.P.M. acknowledges the Portuguese Foundation for Science and Technology for the grant BD/39396/2007 and the MIT-Portugal Program. D.G. acknowledges the Swiss National Science Foundation for a post-doctoral fellowship (PBGEP3-129111). B.P.T. acknowledges an NIR Ruth L. Kirschstein National Research Service Award (F32GM096546).

Appendix A. Figures with essential colour discrimination

Certain figures in this article, particularly Figures 1 and 3–7 are difficult to interpret in black and white. The full colour images can be found in the on-line version, at http://dx.doi.org/10.1016/j.actbio.2014.08.029.

Appendix B. Supplementary data

Supplementary data associated with this article can be found, in the online version, at http://dx.doi.org/10.1016/j.actbio.2014.08.029.

References

[1] MacNeil S. Progress and opportunities for tissue-engineered skin. Nature 2007;445(7130):874–80.
[2] Martin P. Wound healing – aiming for perfect skin regeneration. Science 1997;276(5309):75–81.
[3] Briggaman RA, Wheeler Jr CE. The epidermal–dermal junction. J Invest Dermatol 1975;65(1):71–84.
[4] Groeber F, Holeiter M, Hampel M, Hinderer S, Schenke-Layland K. Skin tissue engineering – in vivo and in vitro applications. Adv Drug Deliv Rev 2011;63(4–5):352–66.
[5] Wassermann D. Severity of burn injuries, epidemiology, prevention, French burn care organization. Pathol Biol (Paris) 2002;50(2):65–73.
[6] Herndon DN, Barrow RE, Rutan RL, Rutan TC, Desai MH, Abston S. A comparison of conservative versus early excision – therapies in severely burned patients. Ann Surg 1989;209(5):547–53.
[7] Papini R. Management of burn injuries of various depths. BMJ 2004;329(7458):158–60.
[8] Shevchenko RV, James SL, James SE. A review of tissue-engineered skin bioconstructs available for skin reconstruction. J R Soc Interface 2010;7(43):229–58.
[9] Bottcher-Haberzeth S, Biedermann T, Reichmann E. Tissue engineering of skin. Burns 2010;36(4):450–60.
[10] Myers SR, Grady J, Soranzo C, Sanders R, Green C, Leigh IM, et al. A hyaluronic acid membrane delivery system for cultured keratinocytes: clinical "take" rates in the porcine kerato-dermal model. J Burn Care Rehabil 1997;18(3):214–22.
[11] Uccioli L. A clinical investigation on the characteristics and outcomes of treating chronic lower extremity wounds using the tissuetech autograft system. Int J Low Extrem Wounds 2003;2(3):140–51.
[12] Caravaggi C, De Giglio R, Pritelli C, Sommaria M, Dalla Noce S, Faglia E, et al. HYAFF 11-based autologous dermal and epidermal grafts in the treatment of noninfected diabetic plantar and dorsal foot ulcers: a prospective, multicenter, controlled, randomized clinical trial. Diabetes Care 2003;26(10):2853–9.
[13] Stark HJ, Willhauck WJ, Mirancea N, Boehnke K, Nord I, Breitkreutz D, et al. Authentic fibroblast matrix in dermal equivalents normalises epidermal histogenesis and dermo-epidermal junction in organotypic co-culture. Eur J Cell Biol 2004;83(11):631–45.
[14] Zhong SP, Zhang YZ, Lim CT. Tissue scaffolds for skin wound healing and dermal reconstruction. Wires Nanomed Nanobi 2010;2(5):510–25.
[15] Martineau L, Doillon CJ. Angiogenic response of endothelial cells seeded dispersed vs. on beads in fibrin gels. Angiogenesis 2007;10(4):269–77.
[16] Nehls V, Schuchardt E, Drenckhahn D. The effect of fibroblasts, vascular smooth muscle cells, and pericytes on sprout formation of endothelial cells in a fibrin gel angiogenesis system. Microvasc Res 1994;48(3):349–63.
[17] Potter MJ, Linge C, Cussons P, Dye JF, Sanders R. An investigation to optimize angiogenesis within potential dermal replacements. Plast Reconstr Surg 2006;117(6):1876–85.
[18] Park D, Kim Y, Kim H, Kim K, Lee YS, Choe J, et al. Hyaluronic acid promotes angiogenesis by inducing RHAMM-TGFbeta receptor interaction via CD44-PKCdelta. Mol Cells 2012;33(6):563–74.
[19] Limat A, Hunziker T, Boillat C, Bayreuther K, Noser F. Post-mitotic human dermal fibroblasts efficiently support the growth of human follicular keratinocytes. J Invest Dermatol 1989;92(5):758–62.
[20] Jia XQ, Colombo G, Padera R, Langer R, Kohane DS. Prolongation of sciatic nerve blockade by in situ cross-linked hyaluronic acid. Biomaterials 2004;25(19):4797–804.
[21] Bulpitt P, Aeschlimann D. New strategy for chemical modification of hyaluronic acid: preparation of functionalized derivatives and their use in the formation of novel biocompatible hydrogels. J Biomed Mater Res 1999;47(2):152–69.
[22] Nociari MM, Shalev A, Benias P, Russo C. A novel one-step, highly sensitive fluorometric assay to evaluate cell-mediated cytotoxicity. J Immunol Methods 1998;213(2):157–67.
[23] Blotta I, Prestinaci F, Mirante S, Cantafora A. Quantitative assay of total dsDNA with PicoGreen reagent and real-time fluorescent detection. Ann Ist Super Sanita 2005;41(1):119–23.
[24] Dupont KM, Sharma K, Stevens HY, Boerckel JD, Garcia AJ, Guldberg RE. Human stem cell delivery for treatment of large segmental bone defects. Proc Natl Acad Sci USA 2010;107(8):3305–10.
[25] Kleinman HK, Philp D, Hoffman MP. Role of the extracellular matrix in morphogenesis. Curr Opin Biotechnol 2003;14(5):526–32.
[26] Bottaro DP, Liebmann-Vinson A, Heidaran MA. Molecular signaling in bioengineered tissue microenvironments. Repar Med Grow Tissues Organs 2002;961:143–53.
[27] Chen WY, Abatangelo G. Functions of hyaluronan in wound repair. Wound Repair Regen 1999;7(2):79–89.
[28] West DC, Hampson IN, Arnold F, Kumar S. Angiogenesis induced by degradation products of hyaluronic acid. Science 1985;228(4705):1324–6.
[29] Yang GP, Lim IJ, Phan TT, Lorenz HP, Longaker MT. From scarless fetal wounds to keloids: molecular studies in wound healing. Wound Repair Regen 2003;11(6):411–8.
[30] West DC, Hampson IN, Arnold F, Kumar S. Angiogenesis induced by degradation products of hyaluronic acid. Science 1985;228(4705):1324–6.
[31] Srinivas A, Ramamurthi A. Effects of gamma-irradiation on physical and biologic properties of crosslinked hyaluronan tissue engineering scaffolds. Tissue Eng 2007;13(3):447–59.
[32] Yamanlar S, Sant S, Boudou T, Picart C, Khademhosseini A. Surface functionalization of hyaluronic acid hydrogels by polyelectrolyte multilayer films. Biomaterials 2011;32(24):5590–9.
[33] Seidlits SK, Khaing ZZ, Petersen RR, Nickels JD, Vanscoy JE, Shear JB, et al. The effects of hyaluronic acid hydrogels with tunable mechanical properties on neural progenitor cell differentiation. Biomaterials 2010;31(14):3930–40.
[34] Lei Y, Gojgini S, Lam J, Segura T. The spreading, migration and proliferation of mouse mesenchymal stem cells cultured inside hyaluronic acid hydrogels. Biomaterials 2011;32(1):39–47.
[35] Pierschbacher M, Hayman EG, Ruoslahti E. Synthetic peptide with cell attachment activity of fibronectin. Proc Natl Acad Sci USA–Biol Sci 1983;80(5):1224–7.
[36] Kisiel M, Martino MM, Ventura M, Hubbell JA, Hilborn J, Ossipov DA. Improving the osteogenic potential of BMP-2 with hyaluronic acid hydrogel modified with integrin-specific fibronectin fragment. Biomaterials 2013;34(3):704–12.
[37] Ghosh K, Ren XD, Shu XZ, Prestwich GD, Clark RAF. Fibronectin functional domains coupled to hyaluronan stimulate adult human dermal fibroblast responses critical for wound healing. Tissue Eng 2006;12(3):601–13.
[38] Jia XQ, Burdick JA, Kobler J, Clifton RJ, Rosowski JJ, Zeitels SM, et al. Synthesis and characterization of in situ cross-linkable hyaluronic acid-based hydrogels with potential application for vocal fold regeneration. Macromolecules 2004;37(9):3239–48.
[39] Bulpitt P, Aeschlimann D. New strategy for chemical modification of hyaluronic acid: preparation of functionalized derivatives and their use in the formation of novel biocompatible hydrogels. J Biomed Mater Res 1999;47(2):152–69.
[40] Yeo Y, Highley CB, Bellas E, Ito T, Marini R, Langer R, et al. In situ cross-linkable hyaluronic acid hydrogels prevent post-operative abdominal adhesions in a rabbit model. Biomaterials 2006;27(27):4698–705.
[41] Snyder SL, Sobocinski PZ. Improved 2,4,6-trinitrobenzenesulfonic acid method for determination of amines. Anal Biochem 1975;64(1):284–8.
[42] Bouhadir KH, Hausman DS, Mooney DJ. Synthesis of cross-linked poly(aldehyde guluronate) hydrogels. Polymer 1999;40(12):3575–84.
[43] Ehrbar M, Rizzi SC, Hlushchuk R, Djonov V, Zisch AH, Hubbell JA, et al. Enzymatic formation of modular cell-instructive fibrin analogs for tissue engineering. Biomaterials 2007;28(26):3856–66.
[44] Ehrbar M, Rizzi SC, Schoenmakers RG, San Miguel B, Hubbell JA, Weber FE, et al. Biomolecular hydrogels formed and degraded via site-specific enzymatic reactions. Biomacromolecules 2007;8(10):3000–7.
[45] Janmey PA, Winer JP, Weisel JW. Fibrin gels and their clinical and bioengineering applications. J R Soc Interface 2009;6(30):1–10.
[46] Leboeuf RD, Raja RH, Fuller GM, Weigel PH. Human fibrinogen specifically binds hyaluronic acid. J Biol Chem 1986;261(27):2586–92.
[47] Bott K, Upton Z, Schrobback K, Ehrbar M, Hubbell JA, Lutolf MP, et al. The effect of matrix characteristics on fibroblast proliferation in 3D gels. Biomaterials 2010;31(32):8454–64.
[48] Beer J, Jonston ER, DeWolf J, Mazurek DF. Mechanics of materials. 5th ed. New York: McGraw-Hill; 2008.
[49] Ahearne M, Yang Y, El Haj AJ, Then KY, Liu KK. Characterizing the viscoelastic properties of thin hydrogel-based constructs for tissue engineering applications. J R Soc Interface 2005;2(5):455–63.
[50] Engler AJ, Sen S, Sweeney HL, Discher DE. Matrix elasticity directs stem cell lineage specification. Cell 2006;126(4):677–89.
[51] Lei YG, Gojgini S, Lam J, Segura T. The spreading, migration and proliferation of mouse mesenchymal stem cells cultured inside hyaluronic acid hydrogels. Biomaterials 2011;32(1):39–47.
[52] Ahmed TAE, Dare EV, Hincke M. Fibrin: a versatile scaffold for tissue engineering applications. Tissue Eng Part B–Rev 2008;14(2):199–215.
[53] Raeber GP, Lutolf MP, Hubbell JA. Mechanisms of 3-D migration and matrix remodeling of fibroblasts within artificial ECMs. Acta Biomater 2007;3(5):615–29.
[54] Lavalle P, Boulmedais F, Ball V, Mutterer J, Schaaf P, Voegel JC. Free standing membranes made of biocompatible polyelectrolytes using the layer by layer method. J Membr Sci 2005;253(1–2):49–56.

[55] Frank DE, Carter WG. Laminin 5 deposition regulates keratinocyte polarization and persistent migration. J Cell Sci 2004;117(Pt 8):1351–63.
[56] Nguyen BP, Gil SG, Carter WG. Deposition of laminin 5 by keratinocytes regulates integrin adhesion and signaling. J Biol Chem 2000;275(41):31896–907.
[57] Rheinwald JG, Green H. Serial cultivation of strains of human epidermal keratinocytes – formation of keratinizing colonies from single cells. Cell 1975;6(3):331–44.
[58] Cukierman E, Pankov R, Stevens DR, Yamada KM. Taking cell–matrix adhesions to the third dimension. Science 2001;294(5547):1708–12.
[59] Shazly TM, Artzi N, Boehning F, Edelman ER. Viscoelastic adhesive mechanics of aldehyde-mediated soft tissue sealants. Biomaterials 2008;29(35):4584–91.
[60] Artzi N, Shazly T, Baker AB, Bon A, Edelman ER. Aldehyde–amine chemistry enables modulated biosealants with tissue-specific adhesion. Adv Mater 2009;21(32–33):3399–403.
[61] Dutta D, Pulsipher A, Luo W, Yousaf MN. Synthetic chemoselective rewiring of cell surfaces: generation of three-dimensional tissue structures. J Am Chem Soc 2011;133(22):8704–13.
[62] Yeo Y, Bellas E, Highley CB, Langer R, Kohane DS. Peritoneal adhesion prevention with an in situ cross-linkable hyaluronan gel containing tissue-type plasminogen activator in a rabbit repeated-injury model. Biomaterials 2007;28(25):3704–13.
[63] Yeo Y, Adil M, Bellas E, Astashkina A, Chaudhary N, Kohane DS. Prevention of peritoneal adhesions with an in situ cross-linkable hyaluronan hydrogel delivering budesonide. J Control Release 2007;120(3):178–85.
[64] Artzi N, Shazly T, Crespo C, Ramos AB, Chenault HK, Edelman ER. Characterization of star adhesive sealants based on PEG/dextran hydrogels. Macromol Biosci 2009;9(8):754–65.